https://doi.org/10.5194/egusphere-2026-4113
Preprint. Discussion started: 14 August 2026

Antecedent groundwater depletion amplifies hydrological drought severity: aquifer-river connectivity and cascading recovery in the 2022 Po Plain extreme event

Shuhan Yang[1], Weijie Zhao[1]*, Giovanni Ravazzani[1], Hui Qian[2345]*, Yixin Liu[234], Zhiming Cao[234]

[1] Department of Civil and Environmental Engineering (D.I.C.A.), Politecnico di Milano, Milano, Italy

[2] School of Water and Environment, Chang'an University, Xi'an 710054, China

[3] Key Laboratory of Subsurface Hydrology and Ecological Effects in Arid Region, Ministry of Education, Chang'an University, Xi'an 710054, China

[4] Key Laboratory of Eco-hydrology and Water Security in Arid and Semi-arid Regions, Ministry of Water Resources, Chang'an University, Xi'an 710054, China

[5] Academy of Yellow River Sciences of Shaanxi Province, Chang'an University, Xi'an 710054, China

** Corresponding authors: weijie.zhao@polimi.it; qianhui@chd.edu.cn (H. Qian)*

https://doi.org/10.5194/egusphere-2026-4113
Preprint. Discussion started: 14 August 2026

Highlights

• Antecedent groundwater depletion strongly amplified the hydrological impact of the 2022 Po River drought.

• Irrigation switched from a groundwater-buffering mechanism to an amplifying feedback under compound drought conditions.

• Recession coefficients increased by 90.7% between 2021 and 2022, exceeding the storage-conditioned expectation.

• Groundwater storage remained below normal long after meteorological conditions had recovered.

• Results reveal multi-year hysteresis in aquifer–river connectivity following extreme drought.

Abstract

The 2022 Po River drought produced a 78% reduction in annual discharge at Pontelagoscuro despite a precipitation deficit of only 20–25%, a discrepancy not attributable to meteorological anomalies alone. Using GRACE-FO groundwater storage anomalies (GWSA), ERA5-Land soil moisture fields, and a 25-year daily discharge record, we show that antecedent aquifer depletion altered aquife-river connectivity, amplifying the hydrological response beyond what meteorological forcing alone would predict.

GWSA had reached −149 mm by August 2021, more than a year before the drought peak. During the 2022 irrigation season, groundwater abstraction substantially exceeded recharge once Alpine-sourced surface water became unavailable, producing the largest single-season storage loss in the 22-year satellite record (−246 mm, Z = −2.32). The recession coefficient k increased by 90.7% between 2021 and 2022, exceeding the storage-dependent trend by 90.5% and consistent with a threshold transition in connectivity near GWSA = −150 mm, a level corresponding to roughly the lowest quintile of the 2002–2024 August GWSA record. Direct runoff collapsed by 72%, leaving baseflow as the dominant hydrograph component.

Recovery proceeded in three tiers: meteorological indices within 8 months, river discharge within 12 months, and soil moisture within 14 months; GWSA had not returned to historically normal levels within the observational record, leaving a period of persistent hydrological drought of at least 7 months undetected by standard precipitation-based indices. Antecedent groundwater

https://doi.org/10.5194/egusphere-2026-4113
Preprint. Discussion started: 14 August 2026

depletion thus alters river discharge sensitivity to meteorological forcing, with recovery in groundwater-dependent irrigated basins extending well beyond the meteorological signal. We propose a diagnostic framework based on GWSA, k, and BFI as an early-warning tool for data-sparse irrigated basins.

Keywords: hydrological drought; groundwater memory; aquifer-river connectivity; baseflow recession; GRACE-FO; Po River; irrigation

https://doi.org/10.5194/egusphere-2026-4113
Preprint. Discussion started: 14 August 2026

1 Introduction

Hydrological droughts in large river systems are rarely a direct expression of contemporaneous meteorological deficits. In basins where groundwater contributes substantially to baseflow, the hydrological response to a given precipitation anomaly depends on the antecedent state of the aquifer: a river underlain by a well-recharged unconfined aquifer can sustain near-normal baseflow through months of below-average precipitation, whereas the same meteorological forcing applied to a pre-depleted aquifer may produce a disproportionate discharge collapse. This storage-dependent sensitivity has been documented in small experimental catchments (Tague and Grant, 2009; Bart and Hope, 2010) and in regional analyses of baseflow persistence (Bloomfield et al., 2019), but its quantitative expression in large, heavily irrigated alluvial basins under extreme drought conditions remains poorly constrained.

Across much of western and central Europe, a combination of winter precipitation deficits, below-average Alpine snowpack, and an intense summer heatwave produced the most severe pan-European drought in at least five centuries by some metrics (Toreti et al., 2022). In the Po Plain of northern Italy, the consequences were extreme: the Po River recorded its lowest flows since systematic measurement began, with discharge at the outlet gauge at Pontelagoscuro falling to approximately 19% of the long-term July mean (160 m^3/s against a July average of 824 m^3/s) in 2022. Agricultural losses across the basin were estimated at several billion euros, and emergency groundwater extraction permits were issued in all four Po Valley regions (ANBI, 2022).

Prior studies of the 2022 event have attributed the discharge anomaly to a combination of reduced winter snowpack (Montanari et al., 2023), elevated evapotranspiration driven by the heatwave (Mastrotheodoros et al., 2020), and the compound nature of the precipitation and thermal anomaly (Buras et al., 2020). Montanari and Ceola (2012) quantified the long-term decline in Po discharge and identified irrigation expansion as a contributing driver. What these studies have not addressed is the role of the antecedent aquifer state in determining the magnitude of the hydrological response: whether the same meteorological forcing applied to an aquifer at its long-term mean would have produced an equally severe discharge anomaly, or whether the multi-year depletion that preceded 2022 was itself a necessary precondition for the observed outcome.

This question has practical implications beyond the Po basin. Across the Mediterranean region and in other semi-arid irrigated systems, groundwater tables have declined progressively over recent

https://doi.org/10.5194/egusphere-2026-4113
Preprint. Discussion started: 14 August 2026

decades under the combined influence of intensifying irrigation demand and increasing drought frequency (Famiglietti, 2014; Rodell et al., 2018; Wada et al., 2010). If antecedent depletion amplifies the hydrological response to meteorological extremes, then the vulnerability of river systems to future droughts may grow faster than would be implied by changes in precipitation alone, and standard meteorological drought indices will systematically underestimate hydrological drought risk during periods of sustained aquifer drawdown.

We address this problem using the 2022 Po Plain drought as a case study. Our specific objectives are: (1) to quantify the antecedent groundwater depletion entering 2022 and its contribution to the total water storage anomaly; (2) to characterise the change in aquifer-river connectivity through analysis of baseflow recession dynamics; (3) to examine the role of irrigation in accelerating depletion during the drought itself; and (4) to quantify the cascading recovery timescales across meteorological, hydrological, and groundwater components. From these analyses we derive a remote-sensing-based diagnostic framework for assessing aquifer–river connectivity state without requiring in-situ groundwater observations.

https://doi.org/10.5194/egusphere-2026-4113
Preprint. Discussion started: 14 August 2026

2 Study area and data

2.1 The Po Plain aquifer-river system

The Po River drains approximately 74,000 km² of northern Italy, extending from the Alpine arc in the north and west to the northern Apennines in the south, and discharging to the Adriatic Sea near the city of Ferrara (Figure 1). The basin encompasses the Po Plain, one of Europe's most intensively cultivated agricultural regions, supporting approximately 35% of Italian agricultural production. Irrigation demands are met primarily from surface water diversions from Alpine tributaries and from the main channel itself, supplemented by groundwater extraction during periods of surface water scarcity.

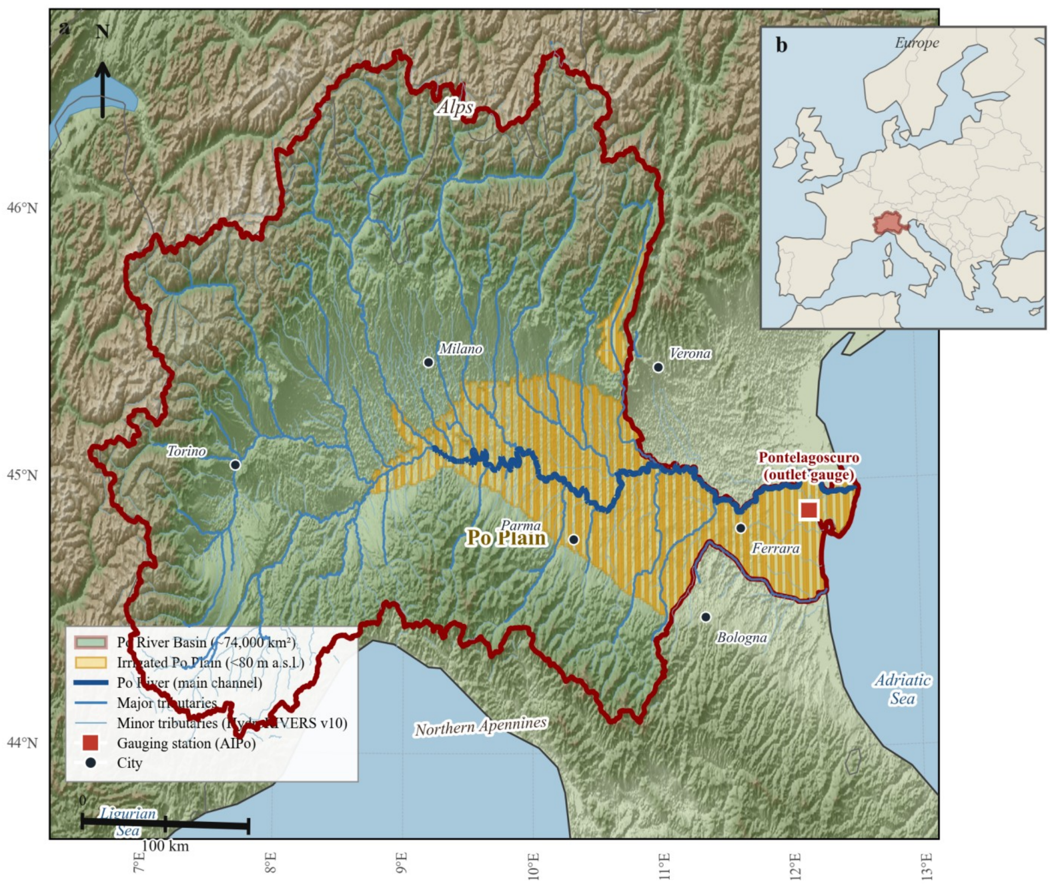

Figure 1. Study area. (a) Po River catchment boundary, river network, and gauging stations at Pontelagoscuro. (b)

https://doi.org/10.5194/egusphere-2026-4113
Preprint. Discussion started: 14 August 2026

Location of the Po basin within Europe. River network from HydroRIVERS (Lehner and Grill, 2013); elevation background from the SRTM digital elevation model (Farr et al., 2007).

The Quaternary sedimentary sequence underlying the Po Plain hosts a multi-layer aquifer system comprising shallow unconfined and deeper semi-confined units (Regione Emilia-Romagna, 2005). The unconfined aquifer, which is hydraulically connected to the Po River through alluvial gravels and sands, is the primary source of baseflow to the main channel. Water table depths are typically 2-10 m below ground level in the valley floor, and seasonal fluctuations of 1-3 m are driven by the balance of irrigation percolation, precipitation, and evapotranspiration. Groundwater abstraction for irrigation is concentrated in the May-September growing season and is responsible for the characteristic summer drawdown of 1-2 m observed in long-term monitoring records.

Daily discharge records are available at two gauging stations operated by the Agenzia Interregionale per il Fiume Po (AIPo): Pontelagoscuro, approximately 100 km from the Adriatic Sea, which integrates runoff from the entire basin. Pontelagoscuro is the primary analysis station. The daily discharge record used in this study spans January 2000 to December 2024, providing 25 years of observations that support multi-year recession analysis and historical baseflow climatology (Arpae-SIMC, 2024).

2.2 Satellite gravimetry: GRACE-FO

Monthly terrestrial water storage anomalies (TWSA) were obtained from the GRACE/GRACE-FO Level-3 monthly land mass grids (Release 06) processed as a three-centre ensemble mean of CSR, GFZ, and JPL spherical harmonic solutions, accessed via Google Earth Engine (collection: NASA/GRACE/MASS_GRIDS/LAND; Landerer et al., 2020). Destriping and 300 km Gaussian smoothing were applied to reduce correlated errors. Direct application of GRACE-FO data to a basin of this size follows the precedent of Carlson et al. (2025), who applied the JPL Mascon solution at comparable resolution across the Po Plain. Gridded scaling factors restored signal power reduced by truncation and filtering. Anomalies are expressed relative to the 2004-2009 baseline period. The dataset extends through late 2023 for the primary analysis; a parallel analysis using the JPL RL06.3 Mascon CRI solution (Wiese et al., 2023) is discussed in Section 5.6. Agreement between the ensemble product and the independent JPL RL06.3 Mascon solution is shown in Figure S2.

https://doi.org/10.5194/egusphere-2026-4113
Preprint. Discussion started: 14 August 2026

GWSA was isolated from TWSA by subtracting contributions from soil moisture storage anomaly (SMSA) and snow water equivalent anomaly (SWEA), both derived from ERA5-Land (Section 2.3). Uncertainty in GWSA was estimated at ±60 mm (95% confidence interval), following the approach of Scanlon et al. (2018), propagating errors from the spherical harmonic ensemble and the ERA5-Land-derived storage components.

2.3 ERA5-Land reanalysis

Monthly ERA5-Land fields (Muñoz-Sabater et al., 2021; Hersbach et al., 2020) were used to derive basin-averaged soil moisture anomalies, actual evapotranspiration, SPEI, and the SMSA and SWEA terms required for GWSA decomposition. Soil moisture was extracted at approximately 9 km spatial resolution across four depth layers spanning 0–289 cm (0–7, 7–28, 28–100, and 100–289 cm). Fields were bilinearly interpolated to the Po catchment boundary and spatially averaged. The reference period for Z-score computation was 2015-2023, using global standardisation (a single μ and σ computed over all months of the reference period rather than calendar-month stratification) to preserve the full seasonal amplitude in the anomaly signal.

SPEI-6 and SPEI-12 were computed using monthly precipitation and potential evapotranspiration derived from ERA5-Land following Vicente-Serrano et al. (2010); Stagge et al. (2015), fitting a three-parameter log-logistic distribution to monthly climate water balance deficits. The 2000-2022 period was used as the calibration window for SPEI standardisation.

2.4 Irrigation data context

No basin-scale irrigation abstraction time series at monthly resolution was available for this study. Irrigation-season groundwater dynamics are therefore characterised indirectly through the GRACE-FO GWSA record, which integrates all storage changes including abstraction. Historical irrigation-season (May-September) GWSA changes were computed for all years with complete observations between 2002 and 2021, providing a statistical baseline against which the 2022 irrigation-season anomaly is assessed. Of the 22-year record, 14 years had complete GRACE/GRACE-FO observations; the remainder were excluded due to data gaps. This approach follows Girotto et al. (2017) and is discussed further in Section 5.2 in the context of the irrigation feedback mechanism documented by Carlson et al. (2025).

https://doi.org/10.5194/egusphere-2026-4113
Preprint. Discussion started: 14 August 2026

3 Methods

3.1 GWSA decomposition

Groundwater storage anomaly was computed as the residual of the total water storage budget:

$$GWSA = TWSA - SMSA - SWEA \quad (1)$$

where TWSA is the three-centre spherical harmonic ensemble, SMSA is the ERA5-Land four-layer soil moisture storage anomaly integrated over the full 0–289 cm profile, and SWEA is the ERA5-Land snow water equivalent anomaly. All terms are expressed as equivalent water height (mm) relative to the 2004-2009 baseline. The freshwater volume deficit was computed as:

$$V = GWSA \times A / 10^3 \quad (2)$$

where A is the catchment area in km^2. GWSA uncertainty, reported at the 95% confidence level, was propagated in quadrature from the spherical harmonic solution error and the ERA5-Land component uncertainties:

$$\sigma_{GWSA}^2 = \sigma_{TWSA}^2 + \sigma_{SMSA}^2 + \sigma_{SWEA}^2 \quad (3)$$

3.2 Baseflow separation

Daily baseflow was separated from total discharge using the Lyne-Hollick recursive digital filter (Lyne and Hollick, 1979; Eckhardt, 2005):

$$Q_b(t) = \alpha\, Q_b(t-1) + [(1-\alpha)/2][Q(t) + Q(t-1)] \quad (4)$$

where $Q_b(t)$ is baseflow at time step t, Q(t) is total discharge, and α is the filter parameter. A value of α = 0.925 was adopted, consistent with prior applications to large lowland rivers (Nathan and McMahon, 1990), and the filter was applied as a triple pass (forward, backward, forward) to reduce phase distortion. The baseflow index was computed as:

$$BFI = \frac{\Sigma Q_b}{\Sigma Q} \quad (5)$$

summed over the full calendar year (Smakhtin, 2001). Direct runoff was computed as $Q_r = Q - Q_b$. Annual mean values of Q, Q_b, Q_r, and BFI are reported in Table 5.

3.3 Baseflow recession analysis

The baseflow recession coefficient k was estimated by fitting an exponential decay model to

https://doi.org/10.5194/egusphere-2026-4113
Preprint. Discussion started: 14 August 2026

uninterrupted declining limbs of the filtered baseflow time series:

$$Q_b(t) = Q_0 \exp(-kt) \quad (6)$$

where Q_0 is the initial baseflow at the start of each recession segment and t is time in days. For 2021 and 2022, the longest continuously declining segment identified within the July-September low-flow window was used. Segments were required to be at least 5 days in length and to show no day-to-day increase exceeding 5% of the preceding value, to exclude rainfall-driven perturbations. Parameters were estimated by ordinary least squares regression on log-transformed baseflow. The half-life of storage was computed as t½ = ln(2)/k.

With the full 2000–2024 discharge record, recession coefficients were computed from measured daily baseflow for all years with sufficient low-flow data (n = 13 years). These values are plotted in Figure 7.

3.4 Soil moisture standardisation

Standardised anomalies for each ERA5-Land soil moisture layer were computed as:

$$Z_i(t) = \frac{\theta_i(t) - \mu_i}{\sigma_i} \quad (7)$$

where θ_i(t) is the monthly volumetric water content for layer i, and μ_i and σ_i are the time-mean and standard deviation computed over the full 2015-2023 reference period. Global standardisation was used to preserve the full seasonal amplitude in the anomaly signal and to maintain consistency with the method used to generate the ERA5-Land soil moisture anomaly fields from which Layers 1 and 4 were independently verified. This reproduction was verified against the original GEE export, yielding a Pearson correlation of r = 1.000. All four layers were derived from a single Google Earth Engine export at scale = 9000 m to ensure inter-layer consistency.

3.5 Drought recovery definition

Recovery was defined separately for meteorological and hydrological variables to reflect the physically distinct memory timescales of each system component. For meteorological variables (precipitation anomaly and SPEI-6), recovery was defined as the first sustained exceedance of the recovery threshold: the first month of at least two consecutive months above the threshold following the drought peak. This criterion is consistent with the drought termination approach of

https://doi.org/10.5194/egusphere-2026-4113
Preprint. Discussion started: 14 August 2026

McKee et al. (1993) and prevents short-lived anomalies from being counted as false recoveries. For hydrological variables (river discharge, soil moisture SMSA, and GWSA), recovery was defined as the final sustained exceedance: the last month in the record that fell below the threshold, after which values remained continuously above it. This stricter criterion accounts for the re-emergence of deficits due to continued extraction or incomplete recharge and follows the approach of Van Loon et al. (2016); Van Loon and Van Lanen (2012) for groundwater-influenced drought recovery.

Recovery thresholds were: precipitation anomaly above zero (3-month moving mean); SPEI-6 above -0.5; river discharge above the calendar-month Q80 threshold (Van Loon, 2016), defined as the flow equalled or exceeded 80% of the time within each calendar month over the 2000–2021 reference period; SMSA above -10 mm; and GWSA above −50 mm, computed as a 3-month moving mean. This GWSA threshold is a conservative lower-bound estimate: the calendar-month 20th percentile threshold recommended by Herbert et al. (2025) was not reached within the observational record. All recovery months are expressed as months elapsed since the September 2022 drought peak. Threshold sensitivity was evaluated using one stricter and one more lenient threshold for each variable; the resulting recovery chronology is summarized in Table S1 and Figure S1.

https://doi.org/10.5194/egusphere-2026-4113
Preprint. Discussion started: 14 August 2026

4 Results

4.1 Meteorological forcing and hydrological response

Basin-averaged annual precipitation in 2022 was approximately 20–25% below the 2015–2021 mean (Figure 2a). SPEI-6 fell below the severe drought threshold (SPEI-6 < -1.5) from approximately March through September 2022, reaching a minimum of approximately −2.0 in July (Figure 2b). Relative to the 2004–2009 baseline, the spring (MAM) precipitation deficit was −65 mm and the summer (JJA) deficit was −84 mm (Table 1). The spring deficit suppressed Alpine snowmelt recharge at the onset of the growing season, while the concurrent summer heatwave elevated evaporative demand across the basin throughout the irrigation period. Together, these two forcings acted on opposite ends of the hydrological cycle: reduced water input from above and increased water loss from below.

Annual mean discharge at Pontelagoscuro fell from 1,109 m^3/s in 2021 to 535 m^3/s in 2022 (−52%), with summer low-flow deficits reaching approximately −78%. Based on the historical precipitation–runoff relationship across 2000–2021, a 20–25% annual precipitation deficit would be expected to produce a discharge anomaly of comparable magnitude. The observed annual deficit of −52% and summer deficit of −78% substantially exceed this expectation, indicating that meteorological forcing alone cannot account for the hydrological response. The sources of this discrepancy are examined in Sections 4.3–4.4.

https://doi.org/10.5194/egusphere-2026-4113
Preprint. Discussion started: 14 August 2026

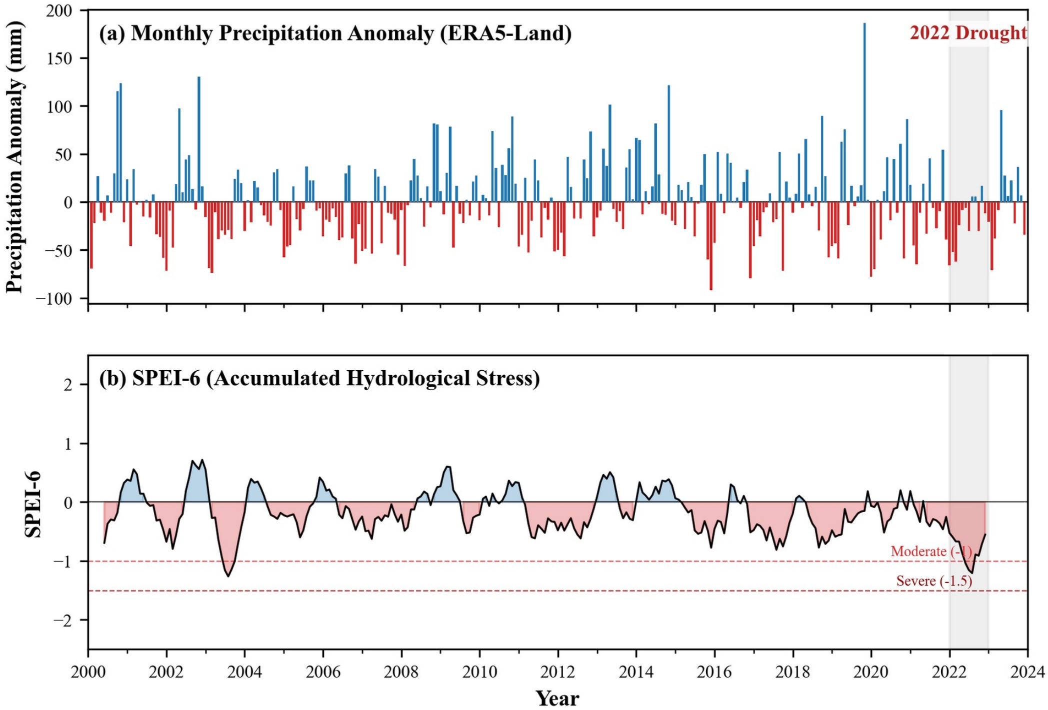

Figure 2. Meteorological forcing, 2000-2022. (a) Monthly basin-averaged precipitation anomaly relative to the 2004-2009 baseline. (b) SPEI-6 time series; dashed lines indicate moderate (-1.0) and severe (-1.5) drought thresholds.

Table 1. *Seasonal terrestrial water storage anomalies (mm) relative to the 2004-2009 baseline from ERA5-Land.*

Season	Baseline 2015-2021 (mm)	2021 Mean (mm)	2022 Mean (mm)	2022 Anomaly (mm)
DJF (Winter)	649	679	631	−18
MAM (Spring)	668	648	603	−65
JJA (Summer)	558	531	473	−84
SON (Autumn)	549	509	490	−58
Annual mean	607	590	547	−60

Note. Anomaly = 2022 Mean - Baseline 2015-2021. All values are spatially averaged over the 74,000 km² basin boundary.

https://doi.org/10.5194/egusphere-2026-4113
Preprint. Discussion started: 14 August 2026

4.2 Vertical propagation of soil moisture deficits

All three shallow layers (Layers 1-3) crossed the −1σ anomaly threshold simultaneously in June 2022, with minimum Z-scores of -2.97, -2.78, and -2.69 for the 0-7, 7-28, and 28-100 cm layers respectively, occurring in July, July, and August (Table 2, Figure 3). The deepest layer (Layer 4, 100-289 cm) crossed the same threshold one month later, in July 2022, and reached its minimum Z-score of -2.48 in October, three months after the near-surface minimum.

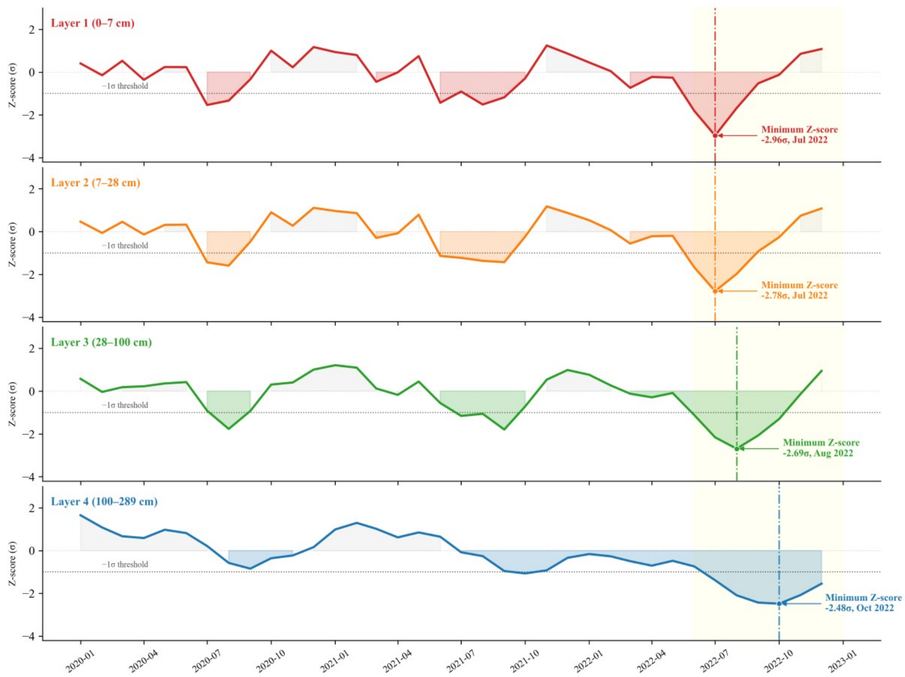

Figure 3. Standardised soil moisture anomalies (Z-score) for four ERA5-Land layers in the Po Basin, January 2020 to December 2022. Z-scores computed using global standardisation over 2015-2023. Yellow shading marks the core drought period (June-December 2022).

Table 2. *Timing of soil moisture anomaly thresholds and evapotranspiration correlation by ERA5-Land depth layer, 2022.*

https://doi.org/10.5194/egusphere-2026-4113
Preprint. Discussion started: 14 August 2026

Layer	Depth (cm)	-1σ threshold crossed	Minimum Z-score	Month of minimum	ET r
Layer 1 (surface)	0-7	Jun 2022	-2.97	Jul 2022	-0.71*
Layer 2	7-28	Jun 2022	-2.78	Jul 2022	—
Layer 3	28-100	Jun 2022	-2.69	Aug 2022	—
Layer 4 (deep)	100-289	Jul 2022	-2.48	Oct 2022	+0.08 (n.s.)

Note. Z-scores computed using global standardisation (μ and σ over 2015-2023; scale = 9000 m, native ERA5-Land resolution). Layer 1 and Layer 4 values independently verified against original GEE export (r = 1.000). ET correlation (Pearson r) with ERA5-Land actual evapotranspiration; * p < 0.01; n.s. = not significant. Surface-to-deep propagation lag = 3 months (July → October 2022).

The surface-to-deep sequence reflects downward diffusion of moisture deficits through the vadose zone under sustained evaporative demand. Layer 1 Z-scores were strongly and negatively correlated with actual evapotranspiration (Pearson $r = -0.71$, $p < 0.01$), consistent with direct evaporative drawdown of near-surface storage. Layer 4 showed no contemporaneous relationship with evapotranspiration ($r = +0.08$, not significant), responding instead to cumulative seasonal water balance on a timescale of weeks to months.

The three-month propagation lag has an important observational implication. Surface-based remote sensing retrievals, which typically sense the upper 5 cm of the soil column, record drought onset in June 2022 and a minimum anomaly in July; they cannot, by design, capture the deepening of deficits through October. In an irrigated alluvial system with shallow groundwater, the vertically integrated moisture deficit substantially exceeds what surface observations alone would suggest, a point that bears directly on the magnitude of the hydrological response described below.

4.3 Antecedent groundwater depletion

The GRACE-FO record shows that the 2022 groundwater depletion was the most severe in the 22-year satellite period, exceeding all prior values at Pontelagoscuro by a substantial margin (Figure 4a). The aquifer was already in a depleted state before the 2022 meteorological drought intensified: GWSA stood at -149 ± 60 mm in August 2021 (Figure 4b), well below the long-term mean. This pre-existing deficit had accumulated through the 2017, 2019, and 2021 growing seasons, each of which recorded below-average recharge, with summer irrigation extraction exceeding subsequent winter recovery in every case.

https://doi.org/10.5194/egusphere-2026-4113
Preprint. Discussion started: 14 August 2026

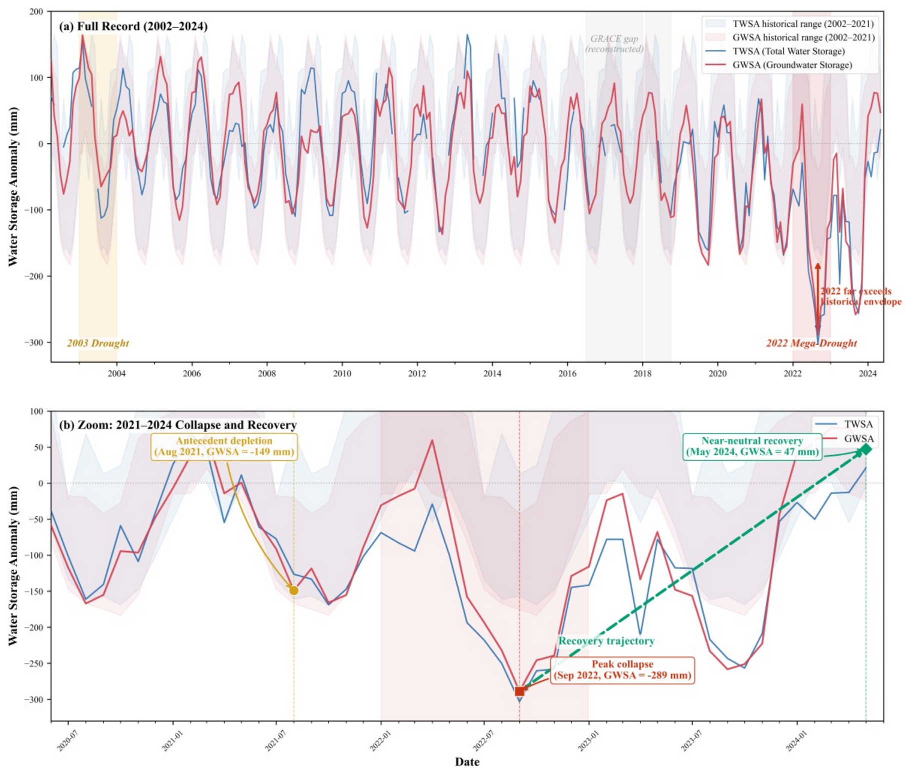

Figure 4. Groundwater storage anomaly in the Po Plain, 2002-2024. (a) Full GRACE-FO record of TWSA (blue) and derived GWSA (red) relative to the 2004-2009 baseline; shading indicates the ±60 mm uncertainty envelope. (b) Zoomed view of 2021-2024, highlighting the antecedent depletion , the September 2022 minimum, and the subsequent recovery trajectory.

Recharge in spring 2022 was further suppressed by below-average snowpack and the MAM precipitation deficit of -65 mm (Table 3), leaving the aquifer at its lowest pre-summer level on record when the heatwave began. GWSA fell from -149 mm in August 2021 to -232 mm in August 2022 before reaching a minimum of -289 ± 60 mm in September 2022, equivalent to approximately 21.4 km^3 below the 2004-2009 baseline. Decomposition of the total water storage anomaly (Table 3) confirms that groundwater change dominated: of the -177 mm TWSA change between August 2021 and August 2022, groundwater accounted for -83 mm, with soil moisture contributing -16 mm and snow water equivalent a small positive term of +10 mm.

https://doi.org/10.5194/egusphere-2026-4113
Preprint. Discussion started: 14 August 2026

Table 3. *Water storage component budget, August 2021 to August 2022 (mm, relative to 2004–2009 baseline).*

Variable	August 2021 (mm)	August 2022 (mm)	Change (mm)
TWSA	−73	−250	−177
SMSA	−6	−22	−16
SWEA	−44	−34	+10
GWSA	−149 ± 60	−232 ± 60	−83
GWSA minimum (Sep 2022)	—	−289 ± 60	—

Note. GWSA uncertainty (±60 mm, 95% CI) from Equation (3). TWSA = SMSA + SWEA + GWSA; minor residuals reflect independent gridded source data. TWSA = total water storage anomaly; SMSA = soil moisture storage anomaly; SWEA = snow water equivalent anomaly; GWSA = groundwater storage anomaly.

The annual water budget obscures an additional depletion mechanism operating within the irrigation season. Under normal conditions, the Po Plain's largely unlined surface-water irrigation system generates substantial percolation recharge, producing a historical mean May-September GWSA change of -145 ± 43 mm (2002-2021; Table 4). In 2022, the corresponding change was -246 mm (Z = -2.32), the largest single-season loss in the observational record and 40 mm below the previous worst year (2005: -206 mm). The trajectory began from an already-depleted May baseline of -43 mm and ended at -289 mm in September (Figure 5b). Where surface water deliveries from Alpine sources are sufficient, percolation offsets a portion of abstraction and buffers aquifer storage, as documented by Carlson et al. (2025). In 2022, the combination of low snowmelt and precipitation deficit curtailed surface-water availability, shifting the net balance toward depletion and eliminating this buffering mechanism.

https://doi.org/10.5194/egusphere-2026-4113
Preprint. Discussion started: 14 August 2026

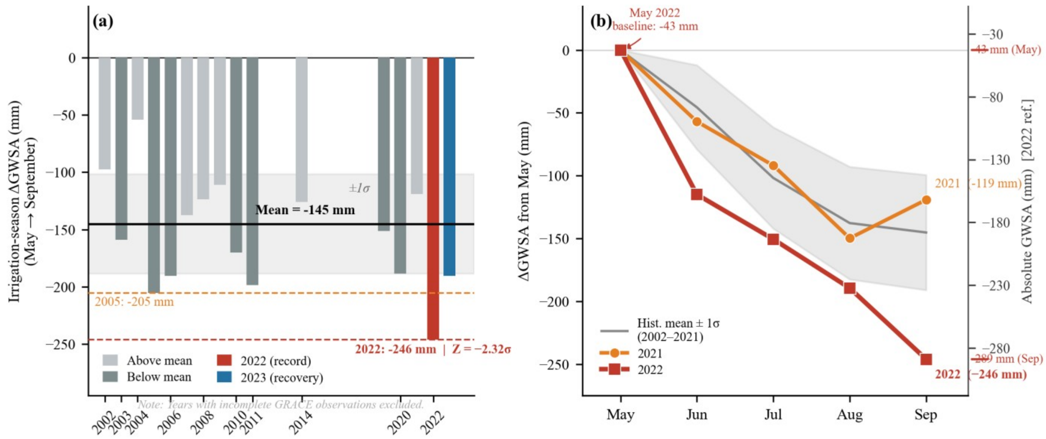

Figure 5. Irrigation-season groundwater storage anomaly in the Po Plain. (a) Annual irrigation-season ΔGWSA (May-September) for all years with complete GRACE/GRACE-FO observations; shading indicates the ±1σ historical range. (b) Monthly GWSA trajectories during the irrigation season for 2021 and 2022, compared with the 2002-2021 historical envelope.

Table 4. *Irrigation season (May-September) groundwater storage anomaly statistics for the Po Plain, 2002-2023.*

Metric	Historical mean 2002-2021	Historical σ	2022 value	Anomaly (Z-score)
GWSA May (mm)	-79	±52	-43	+0.69
GWSA Sep (mm)	-195	±43	-227	-2.19
Irrigation-season ΔGWSA (mm)	-145	±43	-246	-2.32
Previous record low (2005, mm)	—	—	-206	—
Excess depletion vs mean (mm)	—	—	-101	—

Note. Irrigation season defined as May-September. Historical statistics based on n = 14 years with complete May and September GRACE/GRACE-FO observations (years with data gaps excluded). ΔGWSA = GWSA(September) - GWSA(May). The 2022 irrigation-season depletion (-246 mm) is the largest single-season loss in the observational record, exceeding the previous worst year (2005: -206 mm) by 40 mm and lying 2.32σ below the historical mean (Carlson et al., 2025).

4.4 Accelerated baseflow recession and connectivity change

Baseflow separation using the Lyne-Hollick digital filter (α = 0.925, triple pass) yielded annual mean baseflow of 1,019 m^3/s in 2021 and 510 m^3/s in 2022 (-50%), while annual mean direct

https://doi.org/10.5194/egusphere-2026-4113
Preprint. Discussion started: 14 August 2026

runoff contracted from 89.6 to 25.2 m³/s (-72%; Table 5). These annual means are small relative to peak-flow direct runoff (e.g., 1,018 m^3/s during the May 2021 flood peak) because direct runoff is confined to a small number of high-flow days within an otherwise baseflow-dominated annual hydrograph; the year-to-year contrast in this annual mean nonetheless reflects a real reduction in the frequency and magnitude of high-flow events in 2022 relative to 2021. Exponential fitting to the summer low-flow period (Figure 6) gives a recession coefficient k of 0.0144 d^{-1} in 2021 (t½ = 48 days, R^2 = 0.577) and 0.0275 d^{-1} in 2022 (t½ = 25 days, R^2 = 0.799), a factor of 1.9 increase in the rate at which aquifer storage drains to the channel.

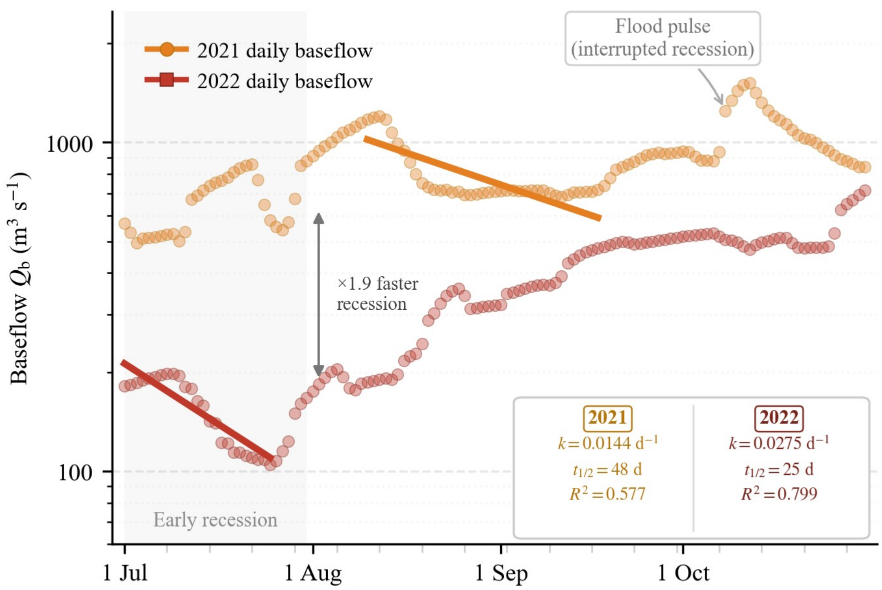

Figure 6. Daily baseflow recession at Pontelagoscuro during the summer low-flow period (1 July-31 October) for 2021 and 2022. Baseflow separated using the Lyne–Hollick digital filter (α = 0.925, triple pass).

Table 5. *Baseflow and recession parameters at Pontelagoscuro, 2021–2024.*

Parameter	2021	2022	2023	2024
Annual mean Q (m³/s)	1106	535	971	2158
Annual mean Qb (m³/s)	1017	510	891	1961
Direct runoff Qr (m³/s)	89.6	25.2	79.8	197

https://doi.org/10.5194/egusphere-2026-4113
Preprint. Discussion started: 14 August 2026

BFI (α = 0.925, triple pass)	0.919	0.953	0.918	0.909
k (d^{-1})	*0.0144*	*0.0275*	*0.0295*	*0.0387*
t½ (days)	48	25	24	18
Recession R^2	0.577	0.799	0.873	0.962
Recession segment	Aug 10–Sep 17	Jul 1–Jul 25	Aug 6–Aug 25	Jul 11–Aug 9
n (days)	39	25	20	30

k values computed from the longest uninterrupted recession segment within July–September using the Lyne–Hollick digital filter (α = 0.925, triple pass). Annual Qb and BFI calculated over the full calendar year. Recession coefficients for 2023 and 2024 exceed the 2022 value despite GWSA remaining near its minimum, indicating multi-year hysteresis in aquifer–river connectivity (Section 5.3).

When plotted against August GWSA (Figure 7), the 2022 recession coefficient lies 90.5% above the value predicted by the log-linear trend fitted to the 13 years with sufficient low-flow data, which has an R^2 of 0.15, placing it well outside the historical recession envelope. Under normal conditions, the recession coefficient scales approximately linearly with storage state, consistent with a well-connected, transmissive aquifer. The departure from this relationship in 2022 is consistent with a threshold transition in aquifer-river connectivity: as GWSA falls below approximately -150 mm, a level corresponding to roughly the lowest quintile of the 2002-2024 August GWSA record, effective transmissivity declines non-proportionally and the hydraulic gradient toward the channel steepens relative to diminishing storage, accelerating drainage.

Measured recession coefficients in 2023 (k = 0.0295 d^{-1}, t½ = 24 days, R^2 = 0.873, n = 20 days) and 2024 (k = 0.0387 d^{-1}, t½ = 18 days, R^2 = 0.962, n = 30 days) remained substantially above the 2021 pre-drought value (0.0144 d^{-1}), with August 2023 GWSA at −233 mm, within 1 mm of the 2022 minimum. The 2024 recession coefficient represents the highest reliably fitted value in the 2000–2024 record. The persistence of elevated k across three consecutive low-flow seasons, at storage levels comparable to the 2022 drought minimum, provides evidence of multi-year hysteresis in aquifer–river connectivity: the drainage rate did not retrace its pre-drought trajectory as storage conditions partially recovered (Table 5).

https://doi.org/10.5194/egusphere-2026-4113
Preprint. Discussion started: 14 August 2026

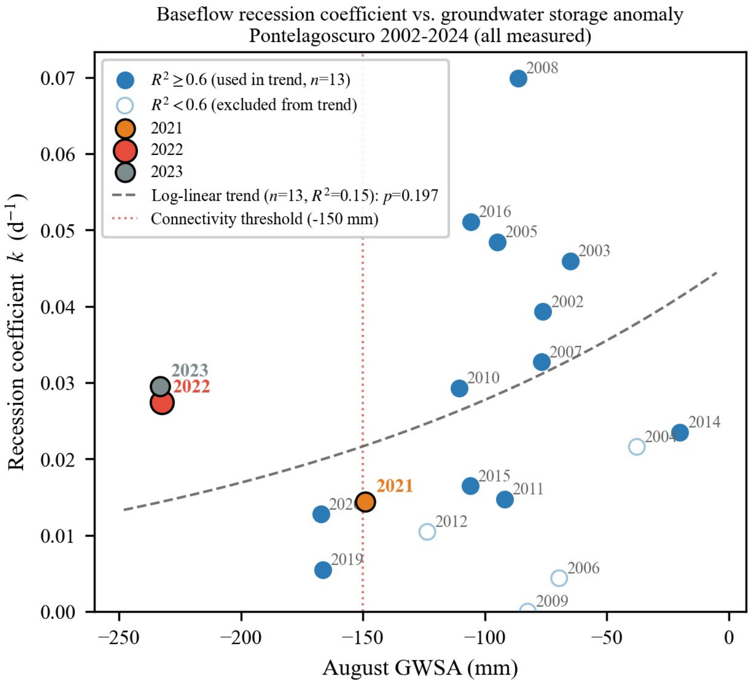

Figure 7. Baseflow recession coefficient k versus August GWSA at Pontelagoscuro, 2002-2023.

4.5 *Recovery timescales across hydrological components*

The recovery trajectory following the September 2022 drought peak proceeded in three distinct tiers (Figure 8). Meteorological indices recovered earliest: basin-averaged precipitation and SPEI-6 both returned above their respective thresholds within 8 months (May 2023), a timescale consistent with observations from comparable European drought events (Van Loon et al., 2016; Bloomfield and Marchant, 2013). River discharge achieved final stable recovery above the calendar-month Q80 threshold within 12 months (September 2023), and soil moisture anomaly (SMSA) within 14 months (November 2023), reflecting the combined memory of the drainage network and unsaturated zone. Groundwater storage (GWSA), assessed against the calendar-month 20th percentile threshold, had not returned to historically normal seasonal levels within the 2024 observational record, with the fixed −50 mm threshold giving a lower-bound estimate of 17 months. This three-tier recovery sequence remained stable under the baseline threshold definitions and persisted across moderate threshold perturbations (Table S1; Figure S1).

https://doi.org/10.5194/egusphere-2026-4113
Preprint. Discussion started: 14 August 2026

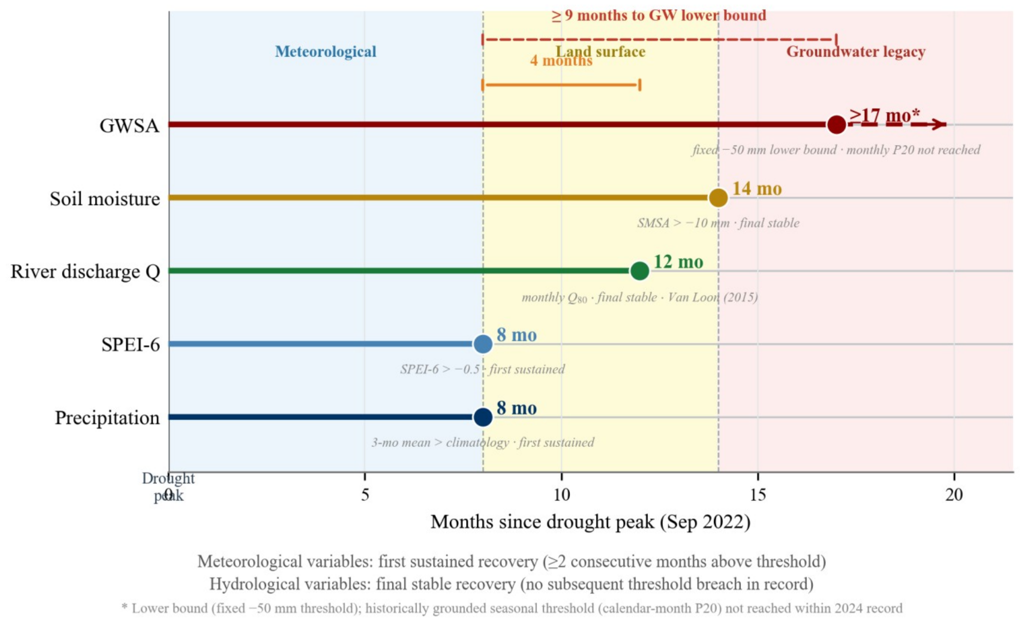

Figure 8. Recovery timeline following the September 2022 drought peak. Each bar extends from the drought peak to the month of recovery for five variables, grouped by recovery tier. Meteorological variables use first sustained recovery; hydrological variables use final stable recovery following Van Loon et al. (2016).

Following meteorological recovery in May 2023, groundwater storage remained below the −50 mm threshold throughout 2023 and, assessed against the calendar-month 20th percentile, had not returned to historically normal levels within the observational record. During this period of at least 7 months after meteorological recovery, during which standard drought indices indicated near-normal or normal conditions while GWSA remained below the -50 mm threshold and, for much of 2023, below -150 mm. During this period, recession coefficients remained elevated and baseflow generation was suppressed despite precipitation returning to near-normal values. The persistence of hydrological drought after meteorological recovery was therefore not driven by continued atmospheric forcing but by the slow process of aquifer recharge.

The divergence in recovery timescales reflects a physical asymmetry between the atmospheric system and the unconfined aquifer. Precipitation anomalies propagate into SPEI-6 on seasonal timescales. Aquifer recovery, by contrast, requires sufficient cumulative recharge to raise the water table to a depth at which hydraulic gradients toward the channel are re-established and baseflow generation resumes at historically normal rates. Until that threshold was crossed, the river could

https://doi.org/10.5194/egusphere-2026-4113
Preprint. Discussion started: 14 August 2026

not respond normally to near-normal precipitation, and the hydrological drought persisted independently of the meteorological state. The lag of at least 7 months between meteorological recovery and the restoration of normal groundwater conditions underscores the inadequacy of precipitation-based indices alone for characterising drought persistence in groundwater-dependent river systems.

https://doi.org/10.5194/egusphere-2026-4113
Preprint. Discussion started: 14 August 2026

5 Discussion

5.1 A forcing-response mismatch driven by antecedent storage deficit

The 78% discharge anomaly at Pontelagoscuro in 2022 cannot be explained by the concurrent meteorological forcing. In years with comparable precipitation deficits drawn from the 2004–2021 record, discharge anomalies were substantially smaller, consistent with the historical precipitation–runoff relationship. The 2022 annual deficit of −52% and summer deficit of −78% both fall well outside the range of prior years with similar precipitation anomalies, indicating that a factor beyond precipitation was governing the magnitude of the hydrological response.

The pre-existing aquifer deficit altered the relationship between rainfall and runoff generation. Under normal storage conditions, the unconfined Po Plain aquifer sustains baseflow by maintaining hydraulic gradients toward the channel throughout the summer low-flow period. When storage is depleted below the connectivity threshold identified here at approximately GWSA = -150 mm, these gradients weaken and the effective transmissivity available to drive baseflow declines non-proportionally. The same precipitation deficit that in a normally charged aquifer would produce a moderate recession instead produces an accelerated one, because the aquifer has less stored water to release and its capacity to transmit that water to the channel has itself been reduced.

This mechanism is consistent with the theoretical framework of storage-dependent baseflow proposed by Tague and Grant (2009) and with empirical observations from Mediterranean catchments (Millares et al., 2012; Oudin et al., 2005), where multi-year dry periods have been shown to reset the storage state sufficiently to alter recession behaviour. What distinguishes the 2022 Po case is the scale of the system and the availability of satellite-based storage observations that allow the storage state entering the drought to be directly quantified rather than inferred from discharge alone.

5.2 Irrigation as an amplifying feedback under extreme conditions

Under normal summer conditions in the Po Plain, the inefficiency of surface-water irrigation generates substantial percolation that recharges the unconfined aquifer (Siebert et al., 2010). Carlson et al. (2025) demonstrated using GRACE-FO and over 1,000 groundwater monitoring wells that this process sustains aquifer levels in irrigated areas through the growing season,

https://doi.org/10.5194/egusphere-2026-4113
Preprint. Discussion started: 14 August 2026

conferring a degree of groundwater resilience that is absent in non-irrigated portions of the basin. Our results show that this mechanism operated in reverse during 2022.

The irrigation-season GWSA change of -246 mm in 2022 was 101 mm more negative than the historical mean and represented the largest single-season depletion in the 22-year record. The underlying shift was one of source substitution: in years when Alpine snowmelt and spring precipitation together sustain surface-water deliveries at near-normal volumes, percolation from canal networks and field irrigation dominates the recharge signal. In 2022, the concurrent failure of snowmelt and spring precipitation curtailed surface-water availability precisely when evaporative demand was elevated by the heatwave, and farmers compensated by intensifying direct groundwater extraction. The result was the largest irrigation-season groundwater storage loss in the observational record, consistent with a net shift from percolation-dominated to abstraction-dominated conditions when surface-water deliveries were unavailable.

This finding adds a temporal dimension to the analysis of Carlson et al. (2025): the groundwater resilience conferred by irrigation percolation depends on the availability of surface water to feed that process. When surface water and precipitation fail simultaneously, as they did in 2022, the irrigation system amplifies rather than buffers the aquifer response. Whether this represents a general vulnerability of surface-water-dependent irrigated systems under compound drought conditions, or a feature specific to the Po Plain's particular irrigation infrastructure, warrants investigation in comparable basins.

5.3 Aquifer-river connectivity and the threshold transition

The 2022 recession coefficient is 90.5% above the value predicted by the GWSA-conditioned trend line fitted to the years with sufficient low-flow data as defined in Methods 3.3, closely matching the 90.7% increase between 2021 and 2022 alone, and this departure is a central finding of this study. A linear storage-discharge relationship would predict a modest increase in k as GWSA declines, reflecting the reduced hydraulic head available to drive flow toward the channel. The observed excess indicates that something qualitatively different occurred in 2022: the system did not simply operate further along the same recession curve, but shifted to a higher-rate regime that is inconsistent with linear drainage of a homogeneous aquifer.

Several physical processes could produce such a transition. As the water table falls below the

https://doi.org/10.5194/egusphere-2026-4113
Preprint. Discussion started: 14 August 2026

elevation of fine-grained interlayers that are common in alluvial sequences, vertical percolation through the unsaturated zone may decouple the deep and shallow portions of the aquifer, reducing the effective saturated thickness contributing to horizontal flow. Alternatively, if portions of the alluvial gravel–channel interface become partially desaturated as the water table drops, the capillary exchange that normally sustains a portion of baseflow may be interrupted (Brunner et al., 2009). Both mechanisms imply a threshold in hydraulic connectivity rather than a smooth continuum, which is consistent with the abrupt departure of the 2022 k value from the historical trend.

Recession coefficients in 2023 (k = 0.0295 d^{-1}, t½ = 24 days, R^2 = 0.873) and 2024 (k = 0.0387 d^{-1}, t½ = 18 days, R^2 = 0.962) remained substantially above the 2021 pre-drought baseline (0.0144 d^{-1}), despite GWSA remaining near its minimum in 2023 and only partially recovering in 2024. The persistence of elevated k across three consecutive low-flow seasons indicates that the threshold transition documented in 2022 was not reversed on a sub-annual timescale. Rather, the data are consistent with a multi-year recovery process in which cumulative recharge must progressively restore the water table to the depth at which normal hydraulic gradients toward the channel are re-established. This interpretation aligns with the GWSA record, in which groundwater storage had not returned to historically normal seasonal conditions within the observational record.

5.4 The lag between meteorological and groundwater recovery

The interval between meteorological recovery in May 2023 and the groundwater lower-bound estimate is robust to threshold choice. GWSA remained below -150 mm throughout 2023, meaning that the hydraulic conditions associated with impaired connectivity persisted for at least 12 months after precipitation returned to near-normal. During this period, baseflow generation was suppressed and river discharge remained suppressed relative to historically normal seasonal levels despite the absence of meteorological drought. An operational drought monitoring system relying solely on SPEI or precipitation anomaly would have declared the drought over in May 2023, approximately 9 months before hydrological conditions had normalised.

The 12-month recovery of river discharge and 14-month recovery of soil moisture fall between the meteorological and groundwater timescales, consistent with both variables integrating signals from multiple system components. Streamflow at Pontelagoscuro reflects a mixture of direct runoff, shallow interflow, and groundwater baseflow; with groundwater still depleted, above-average autumn precipitation in 2023 elevated direct runoff and masked the continued groundwater deficit in the total discharge record. The soil moisture recovery at 14 months reflects the integration of seasonal wetting cycles across the full 0-289 cm profile, with the deep layer (Layer 4) contributing a memory that extends several months beyond the surface signal.

These recovery timescales have practical implications for drought management. Reservoir releases, irrigation allocations, and environmental flow requirements are typically managed on the basis of meteorological outlooks and SPEI-based indices that respond to precipitation on seasonal timescales. In groundwater-dependent systems where aquifer recovery lags meteorological recovery by 9 months or more, management decisions made on the basis of meteorological indices will systematically overestimate the recovery of the hydrological system, potentially leading to premature relaxation of restrictions. Incorporating GWSA monitoring into operational drought assessment frameworks would allow the hidden drought window to be identified and communicated to water managers in near real time.

5.5 A diagnostic framework for data-sparse irrigated basins

The analysis presented here relies on three observable quantities: GWSA from GRACE-FO satellite gravimetry, the baseflow recession coefficient k derived from standard daily discharge records, and the baseflow index BFI computed from the same records. None of these requires in-situ groundwater monitoring, which is absent or poorly distributed across much of the world's irrigated area. The diagnostic framework that emerges from the 2022 Po analysis proposes three indicator thresholds.

GWSA below approximately -150 mm, a level corresponding to roughly the lowest quintile of the 2002-2024 August GWSA record, signals entry into the high-risk zone where threshold connectivity behaviour was observed. An anomalous recession coefficient k that substantially exceeds the GWSA-conditioned expectation provides direct evidence that aquifer–river connectivity has shifted state. An elevated BFI driven by direct runoff collapse rather than by increased groundwater contribution confirms that the system is in the partially decoupled configuration.

When all three indicators are simultaneously present, the diagnostic suggests that the system has

https://doi.org/10.5194/egusphere-2026-4113
Preprint. Discussion started: 14 August 2026

entered a different hydrological regime in which meteorological drought indices will underestimate hydrological drought severity and standard precipitation-based recovery criteria will overestimate recovery speed. The framework is an observational diagnostic that identifies when the conditions for threshold connectivity behaviour have been met; it does not specify the underlying mechanisms.

Whether the -150 mm GWSA threshold identified here is transferable to other irrigated alluvial systems is uncertain and warrants investigation. The Po Plain has shallow water tables (typically 2–10 m), high aquifer transmissivity, and intensive surface-water irrigation infrastructure; basins with deeper water tables or lower irrigation percolation rates may exhibit connectivity thresholds at different storage states. Applying the framework to other Mediterranean and semi-arid irrigated basins with GRACE-FO coverage and discharge records would allow the generality of the threshold concept to be tested and basin-specific calibration curves of k against GWSA to be developed.

5.6 Limitations

Several limitations of this analysis warrant explicit acknowledgement.

The recession analysis draws on a 25-year daily discharge record at Pontelagoscuro (2000–2024), providing measured k values for 13 years with sufficient low-flow data. The Po River is subject to intensive flow regulation through reservoir operations, irrigation diversions, and inter-basin transfers, all of which can interrupt natural recession limbs and bias single-segment exponential fits. The Master Recession Curve approach, designed to average over many segments and therefore less susceptible to this bias, produced an implausible result in 2022 ($k_{2022}/k_{2021} < 1$, $R^2 = 0.43$) and was not adopted. Sensitivity testing confirms that the Lyne–Hollick ratio k_{2022}/k_{2021} is stable across filter parameters (1.88–2.07 for $\alpha = 0.900$–0.950), though absolute k values depend on filter choice and should not be compared directly with estimates from other methods or basins without recomputation on a common basis.

The global standardisation applied to ERA5-Land soil moisture layers conflates the seasonal drying cycle with inter-annual drought anomalies. Over the Po Basin, the seasonal amplitude of soil moisture is 1.9-2.5 times the global standard deviation, so summer Z-scores are systematically more negative than their calendar-month-stratified equivalents by approximately 1.5σ in the

https://doi.org/10.5194/egusphere-2026-4113
Preprint. Discussion started: 14 August 2026

shallow layers. This means that the reported Z-scores reflect the combined effect of seasonal position and inter-annual anomaly, and that an early-onset deficit in winter 2022 which detectable with monthly stratification is masked in the global Z-score record. The relative comparison between 2021 and 2022, which underlies the soil moisture conclusions, is internally consistent because both years are subject to the same seasonal offset, but the absolute Z-score values should be interpreted with this caveat in mind.

Recovery timing estimates are sensitive to the choice of threshold. Varying each threshold by one level shifts the meteorological recovery estimate by at most 1 month, the runoff estimate by up to 3 months, and the groundwater estimate by 1 month. The three-tier cascade structure identified here is preserved under the baseline thresholds but collapses under substantial departures: under strict thresholds the land-surface tier merges with the meteorological tier, and under lenient thresholds groundwater recovery cannot be confirmed within the available record. This recovery lag spans 9-16 months across the range of thresholds tested, with the baseline estimate of 9 months representing the lower bound.

GRACE-FO resolves storage changes at spatial scales of approximately 300 km; sub-basin heterogeneity in aquifer depletion, which is likely given the spatial variability of irrigation intensity across the Po Plain, cannot be captured. Finally, this study cannot distinguish climatically driven storage changes from human-induced depletion in the GWSA record. Attributing the antecedent deficit between these two drivers would require a coupled surface–groundwater model with time-varying irrigation demand, which is beyond the scope of this analysis.

https://doi.org/10.5194/egusphere-2026-4113
Preprint. Discussion started: 14 August 2026

6 Conclusions

Three lines of evidence converge on the same conclusion: the 2022 Po River drought was not a meteorological event that propagated predictably through the hydrological system, but a case in which antecedent aquifer conditions determined the severity of the response.

First, the aquifer entered the 2022 drought season in a substantially pre-depleted state (GWSA = -149 ± 60 mm in August 2021), accumulated through successive dry growing seasons in 2017, 2019, and 2021. This antecedent condition shaped the 2022 hydrological response by reducing the buffering capacity of the aquifer before drought onset: an aquifer entering the 2022 season at its long-term mean storage would have sustained higher hydraulic gradients toward the channel and a materially slower recession. Under present trajectories of groundwater depletion in intensively irrigated basins, antecedent deficits of this scale may become increasingly common, increasing the sensitivity of river discharge to any given meteorological drought.

Second, the irrigation system, which ordinarily buffers summer aquifer drawdown through percolation recharge from surface-water deliveries, operated in reverse during 2022. When Alpine-sourced surface water was unavailable, the irrigation-season groundwater storage loss reached a record margin of −246 mm ($Z = -2.32$), the largest single-season depletion in the 22-year satellite record. This finding qualifies the conclusion of Carlson et al. (2025) that intensive irrigation confers groundwater resilience: that resilience depends on surface water availability and breaks down under compound drought conditions.

Third, the hydrological system had not returned to pre-drought behaviour within three years of the 2022 event. Meteorological indices recovered within 8 months, river discharge within 12 months, and soil moisture within 14 months; groundwater storage remained below historically normal seasonal levels throughout the observational record (lower bound: 17 months). Baseflow recession coefficients in 2023 ($k = 0.0295\ d^{-1}$) and 2024 ($k = 0.0387\ d^{-1}$) exceeded the 2022 drought value ($0.0275\ d^{-1}$), demonstrating that recession behaviour remained anomalous for at least three consecutive low-flow seasons after the drought peak. This multi-year hysteresis in aquifer–river connectivity indicates a structural reorganisation of drainage pathways that persists independently of storage recovery, and cannot be detected by any meteorological drought index. In groundwater-dependent river systems, drought management frameworks that rely solely on meteorological indicators will systematically misidentify the end of drought conditions.

https://doi.org/10.5194/egusphere-2026-4113
Preprint. Discussion started: 14 August 2026

From an observational standpoint, the diagnostic framework proposed here, combining GRACE-FO GWSA with baseflow recession coefficient k and baseflow index BFI derived from standard discharge records, offers a practical means of identifying when aquifer-river connectivity has shifted state and when standard meteorological drought indices are likely to underestimate hydrological drought severity. The framework can be applied in regions where groundwater monitoring is sparse or unavailable, relying instead on satellite gravimetry and standard streamflow records, and is therefore transferable to data-sparse irrigated basins across the Mediterranean and other semi-arid regions where the conditions identified here are increasingly likely to be met.

https://doi.org/10.5194/egusphere-2026-4113
Preprint. Discussion started: 14 August 2026

Code and data availability

GRACE/GRACE-FO Level-3 land mass grids (Release 06) are available via Google Earth Engine (collection: NASA/GRACE/MASS_GRIDS/LAND). JPL RL06.3 Mascon CRI data (Section 5.6) are available from PO.DAAC at https://podaac.jpl.nasa.gov. ERA5-Land data are available from the Copernicus Climate Change Service at https://cds.climate.copernicus.eu. Daily discharge data for Pontelagoscuro are available from the Agenzia Interregionale per il Fiume Po (AIPo) at https://www.agenziapo.it. The river network shown in Fig. 1 is derived from HydroRIVERS (Lehner and Grill, 2013) and the elevation background from the SRTM digital elevation model (Farr et al., 2007); both are public datasets distributed under their own licence terms, which are not CC BY, available at https://www.hydrosheds.org and https://www2.jpl.nasa.gov/srtm/ respectively. All derived data and analysis scripts needed to reproduce every quantitative result and figure in this study are available in a combined repository at https://doi.org/10.5281/zenodo.21933254. The repository is currently accessible to editors and reviewers upon request and will be made publicly available under a CC BY 4.0 licence upon acceptance.

Author contribution

Shuhan Yang conceptualised the study, collected and curated the data, performed the formal analysis, and wrote the original draft. Giovanni Ravazzani contributed to methodology and provided the primary revision of the manuscript. Weijie Zhao and Hui Qian supervised the work as corresponding authors and contributed to writing (review and editing). Yixin Liu and Zhiming Cao provided additional support with data curation and validation. All authors reviewed and approved the final manuscript.

Competing interests

The authors declare that they have no conflict of interest.

Acknowledgements

This work was supported by the China Scholarship Council (CSC No.202406560170). The authors thank the Agenzia Interregionale per il Fiume Po (AIPo) for providing daily discharge records at Pontelagoscuro, and acknowledge the use of GRACE/GRACE-FO data products

https://doi.org/10.5194/egusphere-2026-4113
Preprint. Discussion started: 14 August 2026

distributed via Google Earth Engine and the NASA Physical Oceanography Distributed Active Archive Center (PO.DAAC).

Declaration of Generative AI and AI-assisted Technologies in the Writing Process

During the preparation of this manuscript, the authors used Claude (Anthropic) to generate the graphical abstract and to assist with language editing and revision of the manuscript text. AI-generated graphical content was directly derived from the study's underlying data and figures using reproducible methods. After using these tools, the authors reviewed and edited the content as needed and take full responsibility for the accuracy, originality, and scientific integrity of the manuscript and all figures.

https://doi.org/10.5194/egusphere-2026-4113
Preprint. Discussion started: 14 August 2026

Supplementary material

Table S1. Sensitivity of drought recovery timing to threshold selection. Recovery month is expressed as months elapsed since the September 2022 drought peak. Meteorological variables (precipitation, SPEI-6) use first sustained recovery (≥2 consecutive months above threshold); hydrological variables (river discharge, SMSA, GWSA) use final stable recovery (Van Loon et al., 2016). Thresholds tested are one level stricter and one level more lenient than the baseline values reported in Section 3.5. Values marked '> rec.' indicate that recovery was not confirmed within the available record (December 2023 for discharge and soil moisture; December 2024 for GWSA). The three-tier cascade structure is preserved under the baseline thresholds but collapses under large departures from them.

Figure S1. Sensitivity of drought recovery timing to threshold selection for five hydroclimatic variables at Pontelagoscuro. For each variable, the recovery month is shown under a strict threshold (blue dashed line), the baseline threshold (black solid line), and a lenient threshold (red dashed line), expressed as months since the September 2022 drought peak. Values not reached within the record are indicated by a rightward arrow. SPEI-6 recovery is robust (8–11 months across all thresholds). River discharge recovery is more sensitive (8–14 months). GWSA recovery consistently falls in the third tier (16–17 months under the fixed −50 mm threshold); recovery against the calendar-month 20th percentile was not reached within the observational record.

Figure S2. Comparison of monthly GWSA derived from the three-centre spherical harmonic ensemble (blue solid line; NASA/GRACE/MASS_GRIDS/LAND via Google Earth Engine; Landerer et al., 2020) and the JPL RL06.3 Mascon CRI solution (red dashed line; Wiese et al., 2023) for the Po Basin, 2020–2024. Grey shading indicates the ±60 mm (95% CI) uncertainty envelope on the ensemble product. Both products use ERA5-Land (three-layer, 0–100 cm) soil moisture and snow water equivalent for GWSA isolation, relative to the 2004–2009 baseline. Key differences: (1) timing of the 2022 GWSA minimum (ensemble: September, −289 mm; JPL: August, −294 mm); (2) May 2022 pre-irrigation baseline (ensemble: −43 mm; JPL: −106 mm). ERA5-Land SMSA data end December 2023 for the ensemble product; the 2024 JPL extension uses climatological SMSA and carries an additional uncertainty of ±30 mm.

References

ANBI (Associazione Nazionale Bonifiche Irrigazioni): Rapporto ANBI sulle acque italiane, Associazione

Nazionale Bonifiche Irrigazioni, Rome, Italy, 2022.

Arpae-SIMC (Agenzia regionale per la prevenzione, l'ambiente e l'energia dell'Emilia-Romagna – Servizio IdroMeteoClima): Portata media giornaliera – Pontelagoscuro [Daily mean discharge at Pontelagoscuro], Arpae Emilia-Romagna, Bologna, Italy, available at: https://simc.arpae.it, last access: December 2024.

Bart, R. and Hope, A.: Streamflow response to fire in large catchments of a Mediterranean-climate region using paired-catchment experiments, Journal of Hydrology, 388, 370–378, https://doi.org/10.1016/j.jhydrol.2010.05.016, 2010.

Bloomfield, J. P. and Marchant, B. P.: Analysis of groundwater drought building on the standardised precipitation index approach, Hydrology and Earth System Sciences, 17, 4769–4787, https://doi.org/10.5194/hess-17-4769-2013, 2013.

Bloomfield, J. P., Marchant, B. P., and McKenzie, A. A.: Changes in groundwater drought associated with anthropogenic warming, Hydrology and Earth System Sciences, 23, 1393–1408, https://doi.org/10.5194/hess-23-1393-2019, 2019.

Brunner, P., Cook, P. G., and Simmons, C. T.: Hydrogeologic controls on disconnection between surface water and groundwater, Water Resources Research, 45, W01422, https://doi.org/10.1029/2008WR006953, 2009.

Buras, A., Rammig, A., and Zang, C. S.: Quantifying impacts of the 2018 drought on European ecosystems in comparison to 2003, Biogeosciences, 17, 1655–1672, https://doi.org/10.5194/bg-17-1655-2020, 2020.

Carlson, G., Girotto, M., Wilder, A., and Massari, C.: Intensive irrigation buffers groundwater declines in key European breadbasket, Nature Water, https://doi.org/10.1038/s44221-025-00445-4, 2025.

Eckhardt, K.: How to construct recursive digital baseflow separation filters, Hydrological Processes, 19, 507–515, https://doi.org/10.1002/hyp.5675, 2005.

Famiglietti, J. S.: The global groundwater crisis, Nature Climate Change, 4, 945–948, https://doi.org/10.1038/nclimate2425, 2014.

Farr, T. G., Rosen, P. A., Caro, E., Crippen, R., Duren, R., Hensley, S., Kobrick, M., Paller, M., Rodriguez, E., Roth, L., Seal, D., Shaffer, S., Shimada, J., Umland, J., Werner, M., Oskin, M., Burbank, D., and Alsdorf, D.: The Shuttle Radar Topography Mission, Reviews of Geophysics, 45, RG2004, https://doi.org/10.1029/2005RG000183, 2007.

Girotto, M., De Lannoy, G. J. M., Reichle, R. H., Rodell, M., Draper, C., Bhanja, S. N., and Mukherjee, A.: Benefits and pitfalls of GRACE data assimilation: A case study of terrestrial water storage depletion in India, Geophysical Research Letters, 44, 4107–4115, https://doi.org/10.1002/2017GL072994, 2017.

Hersbach, H., Bell, B., Berrisford, P., Hirahara, S., Horányi, A., Muñoz-Sabater, J., Nicolas, J., Peubey, C., Radu, R., Schepers, D., Simmons, A., Soci, C., Abdalla, S., Abellan, X., Balsamo, G., Bechtold, P., Biavati, G., Bidlot, J., Bonavita, M., De Chiara, G., Dahlgren, P., Dee, D., Diamantakis, M., Dragani, R., Flemming, J., Forbes, R., Fuentes, M., Geer, A., Haimberger, L., Healy, S., Hogan, R. J., Hólm, E., Janisková, M., Keeley, S., Laloyaux, P., Lopez, P., Lupu, C., Radnoti, G., de Rosnay, P., Rozum, I., Vamborg, F., Villaume, S., and Thépaut, J.-N.: The ERA5 global reanalysis, Quarterly Journal of the Royal Meteorological Society, 146, 1999–2049, https://doi.org/10.1002/qj.3803, 2020.

Herbert, C., Döll, P., and Portmann, F. T.: Assessing groundwater drought hazard in groundwater depletion regions: recommendations for large-scale drought early warning systems, Water Resources Research, 61, e2024WR038684, https://doi.org/10.1029/2024WR038684, 2025.

Landerer, F. W., Flechtner, F. M., Save, H., Webb, F. H., Bandikova, T., Bertiger, W. I., Bettadpur, S. V., Byun, S. H., Dahle, C., Dobslaw, H., Fahnestock, E., Harvey, N., Kang, Z., Kruizinga, G. L. H., Loomis, B. D., McCullough, C., Murböck, M., Nagel, P., Paik, M., Pie, N., Poole, S., Strekalov, D., Tamisiea, M. E., Wang, F., Watkins, M. M., Wen, H.-Y., Wiese, D. N., and Yuan, D.-N.: Extending the global mass change data record: GRACE Follow-On instrument and science data performance, Geophysical Research Letters, 47, e2020GL088306, https://doi.org/10.1029/2020GL088306, 2020.

Lehner, B. and Grill, G.: Global river hydrography and network routing: baseline data and new approaches to study the world's large river systems, Hydrological Processes, 27, 2171-2186, https://doi.org/10.1002/hyp.9740, 2013.

Lyne, V. D. and Hollick, M.: Stochastic time-variable rainfall-runoff modelling, in: Proceedings of the Hydrology and Water Resources Symposium, Institution of Engineers Australia, Perth, Australia, 89–93, 1979.

Mastrotheodoros, T., Pappas, C., Molnar, P., Burlando, P., Manoli, G., Parajka, J., Rigon, R., Teuling, A. J., Baldocchi, D., Scott, R. L., and Fatichi, S.: More green and less blue water in the Alps during warmer summers, Nature Climate Change, 10, 155–161, https://doi.org/10.1038/s41558-019-0676-5, 2020.

McKee, T. B., Doesken, N. J., and Kleist, J.: The relationship of drought frequency and duration to time scales, in: Proceedings of the Eighth Conference on Applied Climatology, American Meteorological Society, Anaheim, California, USA, 179–184, 1993.

Millares, A., Gulliver, Z., and Polo, M. J.: Scale effects on the estimation of erosion thresholds through a distributed and physically-based hydrological model, Geomorphology, 153–154, 115–126, https://doi.org/10.1016/j.geomorph.2012.02.016, 2012.

Montanari, A.: Hydrology of the Po River: looking for changing patterns in river discharge, Hydrol. Earth Syst. Sci., 16, 3739–3747, https://doi.org/10.5194/hess-16-3739-2012, 2012..

Montanari, A., Nguyen, H. D., Rubinetti, S., Ceola, S., Galelli, S., Rubino, A., and Zanchettin, D.: Why the 2022 Po River drought is the worst in the past two centuries, Science Advances, 9, eadg8304, https://doi.org/10.1126/sciadv.adg8304, 2023

Muñoz-Sabater, J., Dutra, E., Agustí-Panareda, A., Albergel, C., Arduini, G., Balsamo, G., Boussetta, S., Choulga, M., Harrigan, S., Hersbach, H., Martens, B., Miralles, D. G., Piles, M., Rodríguez-Fernández, N. J., Zsoter, E., Buontempo, C., and Thépaut, J.-N.: ERA5-Land: A state-of-the-art global reanalysis dataset for land applications, Earth System Science Data, 13, 4349–4383, https://doi.org/10.5194/essd-13-4349-2021, 2021.

Nathan, R. J. and McMahon, T. A.: Evaluation of automated techniques for base flow and recession analyses, Water Resources Research, 26, 1465–1473, https://doi.org/10.1029/WR026i007p01465, 1990.

Oudin, L., Hervieu, F., Michel, C., Perrin, C., Andréassian, V., Anctil, F., and Loumagne, C.: Which potential evapotranspiration input for a lumped rainfall-runoff model? Part 2 – Towards a simple and efficient potential evapotranspiration model for rainfall-runoff modelling, Journal of Hydrology, 303, 290–306, https://doi.org/10.1016/j.jhydrol.2004.08.026, 2005.

Regione Emilia-Romagna: Idrogeologia del territorio della Regione Emilia-Romagna, Servizio Geologico, Sismico e dei Suoli, Regione Emilia-Romagna, Bologna, Italy, 2005.

Rodell, M., Famiglietti, J. S., Wiese, D. N., Reager, J. T., Beaudoing, H. K., Landerer, F. W., and Lo, M.-H.: Emerging trends in global freshwater availability, Nature, 557, 651–659, https://doi.org/10.1038/s41586-018-0123-1, 2018.

Save, H., Bettadpur, S., and Tapley, B. D.: High-resolution CSR GRACE RL05 mascons, Journal of Geophysical Research: Solid Earth, 121, 7547–7569, https://doi.org/10.1002/2016JB013007, 2016.

Watkins, M. M., Wiese, D. N., Yuan, D. N., Boening, C., and Landerer, F. W.: Improved methods for observing Earth's time variable mass distribution with GRACE using spherical cap mascons, J. Geophys. Res. Solid Earth, 120, 2648–2671, https://doi.org/10.1002/2014JB011547, 2015.

Wiese, D. N., Yuan, D.-N., Boening, C., Landerer, F. W., and Watkins, M. M.: JPL GRACE and GRACE-FO Mascon Ocean, Ice, and Hydrology Equivalent Water Height CRI Filtered RL06.3Mv04, PO.DAAC, CA, USA, https://doi.org/10.5067/TEMSC-3MJ634, 2023.

Scanlon, B. R., Zhang, Z., Save, H., Sun, A. X., Schmied, H. M., van Beek, L. P. H., Wiese, D. N., Wada, Y., Long, D., Reedy, R. C., Longuevergne, L., Döll, P., and Bierkens, M. F. P.: Global models underestimate large decadal declining and rising water storage trends relative to GRACE satellite data, Proceedings of the National Academy of Sciences, 115, E1080–E1089, https://doi.org/10.1073/pnas.1704665115, 2018.

Siebert, S., Burke, J., Faures, J. M., Frenken, K., Hoogeveen, J., Döll, P., and Portmann, F. T.: Groundwater use for irrigation – a global inventory, Hydrology and Earth System Sciences, 14, 1863–1880, https://doi.org/10.5194/hess-14-1863-2010, 2010.

Smakhtin, V. U.: Low flow hydrology: a review, Journal of Hydrology, 240, 147–186, https://doi.org/10.1016/S0022-1694(00)00340-1, 2001.

Stagge, J. H., Tallaksen, L. M., Gudmundsson, L., Van Loon, A. F., and Stahl, K.: Candidate distributions for climatological drought indices (SPI and SPEI), International Journal of Climatology, 35, 4027–4040, https://doi.org/10.1002/joc.4267, 2015.

Tapley, B. D., Bettadpur, S., Ries, J. C., Thompson, P. F., and Watkins, M. M.: GRACE measurements of mass variability in the Earth system, Science, 305, 503–505, https://doi.org/10.1126/science.1099192, 2004.

Tague, C. L. and Grant, G. E.: Groundwater dynamics mediate low-flow response to global warming in snow-dominated alpine regions, Water Resources Research, 45, W07421, https://doi.org/10.1029/2008WR007179, 2009.

Toreti, A., Bavera, D., Acosta Navarro, J., Cammalleri, C., de Jager, A., Di Ciollo, C., Hrast Essenfelder, A., Maetens, W., Magni, D., Masante, D., Mazzeschi, M., McCormick, N., and Spinoni, J.: Drought in Europe Summer 2022, Publications Office of the European Union, Luxembourg, https://doi.org/10.2760/264241, 2022.

Van Loon, A. F. and Van Lanen, H. A. J.: A process-based typology of hydrological drought, Hydrology and Earth System Sciences, 16, 1915–1946, https://doi.org/10.5194/hess-16-1915-2012, 2012.

https://doi.org/10.5194/egusphere-2026-4113
Preprint. Discussion started: 14 August 2026

Van Loon, A. F., Gleeson, T., Clark, J., Van Dijk, A. I. J. M., Stahl, K., Hannaford, J., Di Baldassarre, G., Teuling, A. J., Tallaksen, L. M., Uijlenhoet, R., Hannah, D. M., Sheffield, J., Svoboda, M., Verbeiren, B., Wagener, T., Rangecroft, S., Wanders, N., and Van Lanen, H. A. J.: Drought in the Anthropocene, Nature Geoscience, 9, 89–91, https://doi.org/10.1038/ngeo2646, 2016.

Wada, Y., van Beek, L. P. H., van Kempen, C. M., Reckman, J. W. T. M., Vasak, S., and Bierkens, M. F. P.: Global depletion of groundwater resources, Geophysical Research Letters, 37, L20402, https://doi.org/10.1029/2010GL044571, 2010.

Vicente-Serrano, S. M., Beguería, S., and López-Moreno, J. I.: A multiscalar drought index sensitive to global warming: The Standardized Precipitation Evapotranspiration Index, Journal of Climate, 23, 1696–1718, https://doi.org/10.1175/2009JCLI2909.1, 2010.